Basic Physics Predicts Stronger High Cloud Radiative Heating With Warming

B. Gasparini, G. Mandorli, C. Stubenrauch, A. Voigt

Geophysical Research Letters

RESEARCH LETTER
10.1029/2024GL111228

Basic Physics Predicts Stronger High Cloud Radiative Heating With Warming

B. Gasparini[1], G. Mandorli[2], C. Stubenrauch[2], and A. Voigt[1]

[1]Department of Meteorology and Geophysics, University of Vienna, Vienna, Austria, [2]Laboratoire de Météorologie Dynamique/Institut Pierre-Simon Laplace, LMD/IPSL, Sorbonne Université, École Polytechnique, CNRS, Paris, France

Key Points:

- Cloud radiative heating intensifies as clouds move upward
- We show evidence for cloud radiative heating intensification in models of multiple complexity and satellite retrievals
- We develop a simple theory to predict these changes in cloud radiative heating

Supporting Information:

Supporting Information may be found in the online version of this article.

Correspondence to:

B. Gasparini,
blaz.gasparini@univie.ac.at

Citation:

Gasparini, B., Mandorli, G., Stubenrauch, C., & Voigt, A. (2024). Basic physics predicts stronger high cloud radiative heating with warming. *Geophysical Research Letters*, *51*, e2024GL111228. https://doi.org/10.1029/2024GL111228

Received 5 JUL 2024
Accepted 4 DEC 2024

Abstract Radiative heating of clouds, particularly those in the upper troposphere, alters temperature gradients in the atmosphere, affecting circulation and precipitation in today's and future climates. However, the response of cloud radiative heating to global warming remains largely unknown. We study changes to high cloud radiative heating in a warmer climate, identify physical mechanisms responsible for these changes, and develop a theory based on well-understood physics to predict them. Our approach involves a stepwise procedure that builds upon a simple hypothesis of an upward shift in cloud radiative heating at constant temperature and gradually incorporates additional physics. We find that cloud radiative heating intensifies as clouds move upward, suggesting that the role of high clouds in controlling atmospheric circulations increases in a warmer climate.

Plain Language Summary Clouds are moving higher up as the world warms, and this affects local temperatures. When clouds change altitude, the amount of air molecules around them changes too, and that's the key process that drives this change. We show evidence supporting this process using a combination of various atmospheric model simulations and satellite observations. This effect is most evident in high clouds, which experience large altitude shifts as surface temperatures rise. We can predict these changes if we understand how clouds impact local temperatures in today's climate. However, that's still uncertain, and making a solid prediction with our current knowledge is challenging.

1. Introduction

The interactions of ice crystals with radiative fluxes in tropical high clouds alter heating within the atmosphere (Ackerman et al., 1988; Dinh et al., 2023; Voigt et al., 2024), a quantity known as cloud radiative heating (CRH). CRH is defined as:

$$\frac{dT}{dt} = \frac{1}{\rho c_p} \frac{d(F_{all-sky} - F_{clear-sky})}{dz} \quad (1)$$

where F is the radiative flux in W m^{-2}, ρ is the local density of air in kg m^{-2}, c_p is the specific heat of air, and z is the altitude in m. CRH influences the temperature structure in the upper troposphere and modulates the strength and position of tropical and extratropical circulations, including the intertropical convergence zone, monsoons, and midlatitude storm tracks (Byrne & Zanna, 2020; Ceppi & Shepherd, 2017; Li et al., 2015; Voigt & Shaw, 2015). Additionally, CRH plays a major role in atmospheric energy balance and precipitation (Harrop & Hartmann, 2016b; Li et al., 2015; Medeiros et al., 2021; Voigt et al., 2021), ENSO (Rädel et al., 2016), tropical cyclone intensification (Ruppert et al., 2020), and convective self-aggregation (Muller et al., 2022; Pope et al., 2021). While both low and high clouds lead to strong CRH, high-cloud CRH strongly controls large-scale circulation patterns by directly affecting temperatures in the upper troposphere (Haslehner et al., 2024; Lohmann & Roeckner, 1995; Ramanathan et al., 1983). It also influences high cloud amount, properties, radiative impact, and their diurnal cycle (Gasparini et al., 2019, 2022; Harrop & Hartmann, 2016a; Hartmann et al., 2018; Wall et al., 2020).

Changes in climate and clouds lead to changes in CRH that influence the atmospheric circulation response to warming in both the tropics (Albern et al., 2018; Voigt & Shaw, 2015) and extratropics. Studies using both idealized and realistic global model setups suggest that more than half of the model spread in the midlatitude jet response is caused by changes in CRH (Ceppi & Hartmann, 2016; Ceppi & Shepherd, 2017; Li et al., 2019; Voigt

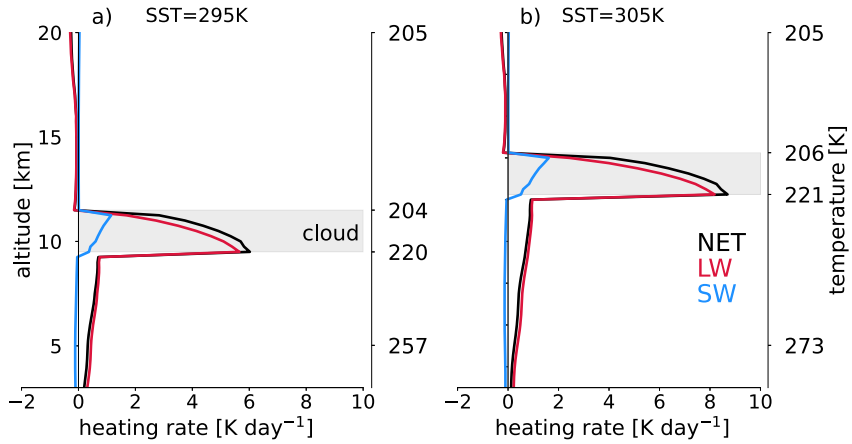

Figure 1. Cloud radiative heating of an idealized cloud over an ocean surface with a temperature of 295 K (a) and 305 K (b) calculated with a radiative transfer model. Both clouds have a COD of 1. Figure S1 in Supporting Information S1 shows the same quantities using pressure coordinates.

& Shaw, 2015, 2016). Changes in high-cloud CRH strongly influence how large-scale circulation patterns react to global warming (Voigt & Albern, 2019). These changes affect the regional manifestation of climate change by determining the location of precipitation associated with storm tracks and the characteristics of the tropical rain belts.

High clouds are expected to remain at a nearly constant temperature over a wide range of climates, known as the fixed anvil temperature (FAT) mechanism (Hartmann & Larson, 2002). While FAT or its variants (Bony et al., 2016; Thompson et al., 2017) were empirically shown to hold in climate projections, broad range of tropical-like climates (Singh & O'Gorman, 2015; Seeley et al., 2019), tropical interannual variability (Zelinka & Hartmann, 2011; Li et al., 2012; C. Zhou et al., 2014; Höjgård-Olsen et al., 2022; Takahashi et al., 2024), their underlying assumptions have recently been challenged (Seeley et al., 2019). Nevertheless, changes in high clouds and relative humidity in CMIP6 models can be predicted by isothermal vertical shifts following FAT and diluted moist adiabats (Po-Chedley et al., 2019).

Despite numerous studies on tropospheric expansion and changes in clear-sky cooling rates with surface warming (Hartmann et al., 2022; Jeevanjee & Fueglistaler, 2020; Knutson & Manabe, 1995; Mitchell & Ingram, 1992), responses of CRH to global warming remain largely unknown.

In this study, we analyze how CRH changes in a warmer climate, identify physical mechanisms responsible for these changes, and develop a theory based on well-understood physics to predict them. To develop our theory of CRH change, we draw on multiple lines of evidence. First, we conduct radiative transfer simulations of an idealized high cloud. Next, we perform simulations in radiative-convective equilibrium (RCE) conditions over a wide range of climates using the System for Atmospheric Modeling (SAM) cloud-resolving model (Khairoutdinov & Randall, 2003). Then, we analyze data from multiple models from the Radiative Convective Equilibrium Model Intercomparison Project (RCEMIP) data set (Wing et al., 2018, 2020a). Finally, we support our theory with a 15-year satellite-derived CRH data set (Stubenrauch et al., 2021, 2023).

2. Data and Methods

2.1. Radiative Transfer Calculations

The radiative calculations are performed with the RRTMG radiative transfer model (Iacono et al., 2008; Mlawer et al., 1997). We initialize the atmospheric profiles of temperature and humidity to equilibrated model-computed RCE conditions at the given SST (295 and 305 K). Both SST cases contain a uniform ice cloud layer with a geometric thickness of 2 km, with a constant ice water content (IWC) of 0.005 g m^{-3}, and a cloud optical depth (COD) of 1 (Figure 1), similar to most frequently observed high clouds (Sokol & Hartmann, 2020). Cloud properties remain the same in the 295 and 305 K simulations, while cloud temperatures remain approximately

unchanged, warming slightly due to the coarse vertical grid spacing (Figure 1). Therefore, the cloud in the 305 K simulation is located 2.75 km higher than the cloud in the 295 K case.

2.2. Simulations

2.2.1. SAM CRM

We perform 11 SAM simulations in RCE at SSTs ranging between 265 and 315 K in 5 K intervals, following the RCE_small RCEMIP experiment specifications (Wing et al., 2018). For the analysis, we consider the averages of the last 25 out of 100 days of the simulation. For more information on SAM, see Text S1 in Supporting Information S1.

2.2.2. RCEMIP

We use the RCEMIP data (Wing et al., 2018, 2020a) from the RCE_large295 and RCE_large305 simulations. Simulations from 18 of the 30 models or model versions available at the time of our initial data download provide the output needed to compute CRH profiles, that is, both clear-sky and cloudy-sky radiative profiles (Table S1 in Supporting Information S1). Our work focuses on the 13 CRM models; GCM results are discussed in Section 4.

2.3. Synergetic Cloud and CRH Data Set (CIRS-ML)

We use a 15-year (2004–2018) 3D cloud and radiative heating data set developed by Stubenrauch et al. (2021), described in the Text S2 in Supporting Information S1. It expands in time and space the radiative heating rates from 2B-FLXHR-LIDAR (Henderson et al., 2013) using deep learning applied to cloud, atmospheric, and surface properties from AIRS-CIRS satellite data (Stubenrauch et al., 2017) and ERA-Interim reanalyses (Dee et al., 2011). We use data for the tropical band between 15°S and 15°N only.

2.4. Tropical Sea Surface Temperature Data

We use monthly mean SST data from the National Oceanic and Atmospheric Administration Optimum Interpolation Sea Surface Temperature version 2 data set (Huang et al., 2021) from July 2004 to June 2018 between 15°S and 15°N. The tropical mean temperature is obtained by averaging over latitude and longitude. Subsequently, annual means are computed from July to June to capture the effect of ENSO, which peaks during the boreal winter.

3. Results

3.1. CRH Response of an Idealized Cloud Shift

In the following, we highlight that CRH increases as clouds move to higher altitudes, driven by changes in air density. An upward shift would intuitively, given no change in high cloud properties, lead to a vertically shifted CRH profile with no change in CRH magnitude.

Figure 1a shows the computed profile of net, shortwave (SW), and longwave (LW) CRH for a 2 km thick cloud with a COD of 1. The cloud is embedded in a moisture and temperature environment that represents an equilibrated climate state at 295 K SST. The major CRH contribution comes from the LW absorption which generates maximum heating at the cloud base.

Figure 1b shows the same cloud with nearly the same cloud temperature over an ocean surface at 305 K. Its geometric extent, ice properties (IWC, ice water path, ice crystal size), and COD are set to be the same as in the 295 K simulation to isolate the effect of a pure upward cloud shift. The two clouds are prescribed in a way to maintain a nearly constant temperature. The cloud at SST of 305 K is therefore shifted upward by 2.75 km compared to the cloud at 295 K SST. Remarkably, the CRH increases by about 50% in the warmer simulation despite no changes in cloud properties.

Equation 1 consists of the terms $\frac{1}{\rho}$ and dF/dz, both of which can change with the upward cloud shift over warmer surface temperatures. Changes in the $\frac{1}{\rho}$ term at peak CRH, computed as $100 \times \frac{1/\rho_{305} - 1/\rho_{295}}{1/\rho_{295}}$, explain about 87% of the change in LW CRH and 97% in SW CRH, defined as $100 \times \frac{(dT/dt)_{305} - (dT/dt)_{295}}{(dT/dt)_{295}}$ (Table S2 in Supporting

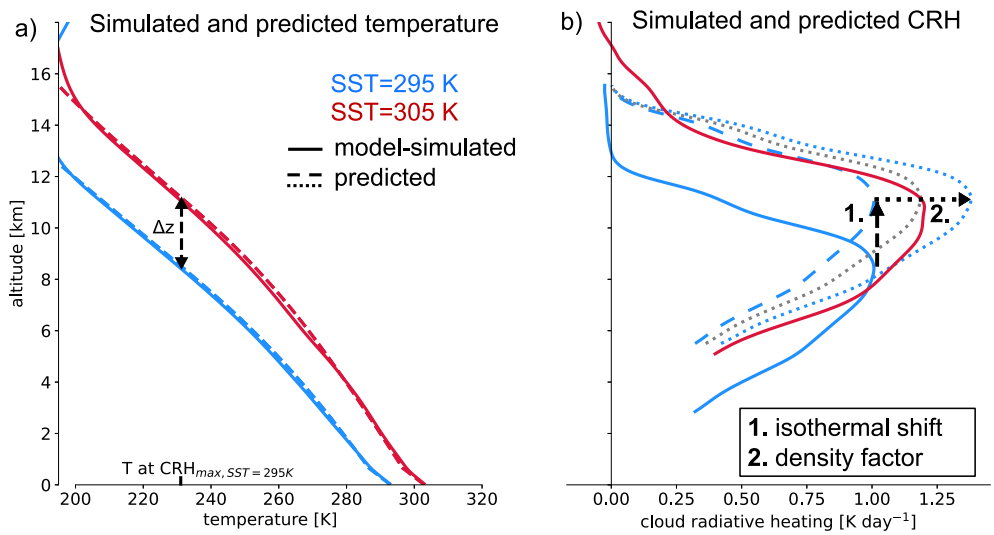

Figure 2. (a) SAM model simulated temperature profiles for SSTs of 295 and 305 K (solid lines) and the corresponding diluted moist adiabats (dashed lines). The vertical shift of peak CRH (Δz) is determined based on the assumption of isothermal conditions at peak CRH. (b) CRH profiles for the reference and warmer climate states (solid lines). The dashed blue line is the 295 K CRH shifted by the predicted Δz. The dotted blue line is the CRH profile based on the predicted Δz and the density factor. The dotted gray line is the prediction multiplied by a factor considering the simulated decrease in peak cloud fraction.

Information S1). The residual change in LW CRH is explained by the increase in LW emission reaching the cloud base due to higher surface temperatures. The decrease in density also makes the atmospheric column above the cloud top more transparent in the warmer simulation. As a result, more SW radiation reaches the cloud top, leading to a slight increase in SW CRH.

In summary, CRH (Equation 1) is determined by two terms: (a) the $\frac{1}{c_p \rho}$ term, determined by air density and (b) the $\frac{dF}{dz}$ term, controlled by cloud properties. As a cloud moves to higher altitudes, air density decreases, increasing the magnitude of term (a) and thus, assuming no change in cloud properties, increasing the magnitude of CRH due to its inverse proportionality with density. While radiatively important boundary layer clouds remain at nearly the same altitude in warmer (or colder) climates, free tropospheric clouds shift robustly in altitude with warming (Sherwood et al., 2020). Upward shifts are largest for high clouds, which are therefore expected to experience the largest changes in air density. The change in CRH is not only caused by a simple altitude shift of the CRH profile but also by a density-driven increase in CRH magnitude.

3.2. Prediction of CRH Profiles

We reproduce the mean temperature profile obtained from the SAM simulation at 295 K using the spectral plume model (W. Zhou & Xie, 2019) (see also Text S3 in Supporting Information S1). Next, we find the temperature at the peak CRH level of the 295 K simulation. The CRH peak corresponds approximately to the average temperature of the cloud base where net heating is maximized due to the dominant LW absorption component (see Figure 1). We now assume that the temperature at peak CRH is independent of SST to find the altitude of the peak CRH at other climate conditions. This allows us to determine the vertical displacement Δz between the CRH peaks in the colder and warmer simulations, shown in Figure 2a for a 10 K temperature change. As we focus on high clouds, we only consider CRH at temperatures colder than 273 K where cloud ice is present. The same method is applied to the RCEMIP multimodel data to predict CRH at 305 K and assuming the 295 K profiles as the reference, known, climate state.

The simulated 295 K SAM temperature profile in Figure 2b is moved upward based on the predicted vertical shift Δz, represented by the dashed blue line. The dotted CRH profile adds the predicted density adjustment factor defined as:

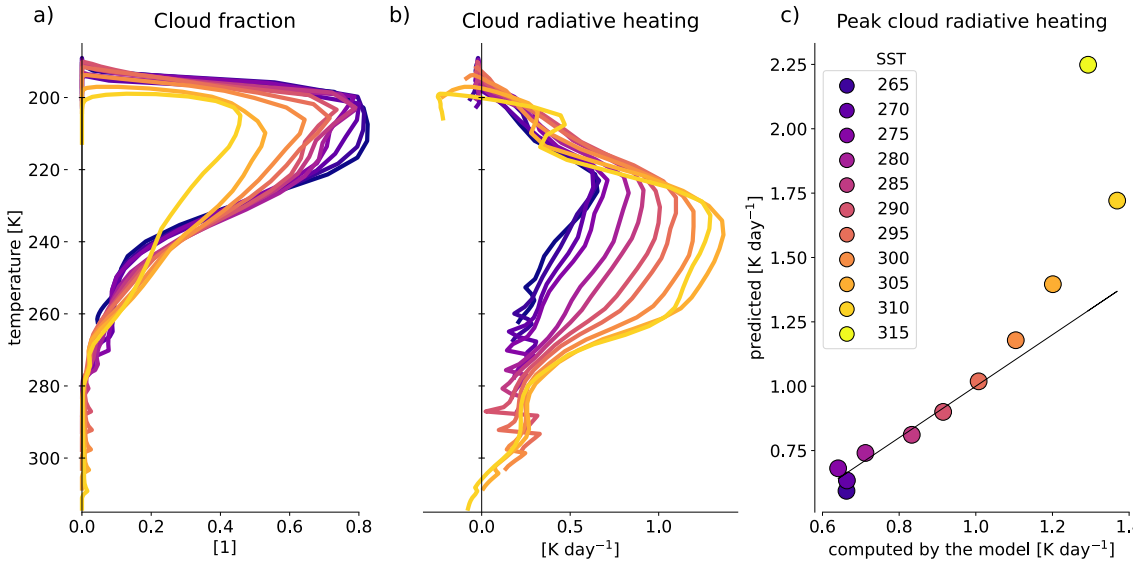

Figure 3. (a) SAM model-simulated cloud fraction and (b) CRH profiles. (c) Prediction of peak CRH compared with SAM model-simulated values over an extended temperature range. The CRH prediction in (c) is based on the model-simulated CRH at 295 K and the predicted changes in density. The black line represents the 1:1 line between computed and predicted CRH.

$$\rho_{corr,pred}(z) = \rho_{295}(z + \Delta z)/\rho_{295}(z) \quad (2)$$

The $\rho_{corr,pred}(z)$ is calculated purely from the estimated vertical shift Δz and the density profile in the colder simulation.

The prediction in Figure 2b overestimates the peak CRH due to a 10% decrease in peak cloud fraction in between the 305 and 295 K simulations (Figure 3a). Multiplying the prediction with a factor considering the decrease in the simulated peak cloud fraction improves the agreement, as shown by the gray dotted line (Figure 2b).

3.3. CRH Intensification and Its Prediction in RCE Simulations

We conduct SAM model simulations in RCE over a wide range of SSTs from 265 to 315 K, extending from snowball-Earth-like climates to near-hothouse climates. All climate conditions result in a prominent peak in cloud fraction in the upper troposphere that becomes less pronounced in warmer simulations while maintaining a roughly constant temperature (Figure 3a and Figure S3a in Supporting Information S1). Similarly, CRH peaks in the upper troposphere below the peak cloud fraction near the cloud base (Figure 3b). Unlike cloud fraction, the CRH gradually increases in magnitude. Interestingly, the variation of the domain-averaged $\frac{dF}{dz}$ term is small relative to density variations for all but the highest SST simulation (Table S3 in Supporting Information S1). The change in temperature at peak CRH varies little compared to changes in SST over the simulated range of climates (Figure S3b in Supporting Information S1). We consider it therefore fixed for our prediction of the $\frac{1}{c_p\rho}$ term.

We now demonstrate that the response of the upper tropospheric CRH can be reliably predicted from the profile of CRH in the reference, present-day-like 295 K climate following well-understood physics of tropical clouds and convection extending the procedure explained in Section 2.5 to a broader range of climates (see also Text S3 in Supporting Information S1). The predicted CRH changes are based solely on the reference climate, without the need for knowledge of warmer or colder climate states. The prediction is biased for simulations at SSTs > 295 K with large peak cloud fraction changes (Figures 3a and 3c).

Nevertheless, our simple method is skillful in predicting the peak upper tropospheric CRH for simulations with SSTs up to 30 K colder and 15 K warmer than the reference simulation at 295 K SST (correlation coefficient of 0.98, root mean square error of 0.13) (Figure 3c). This proves the predictive power of our method, which relies on basic physics, and demonstrates the inversely proportional relationship between air density and CRH accross a wide range of surface climate conditions.

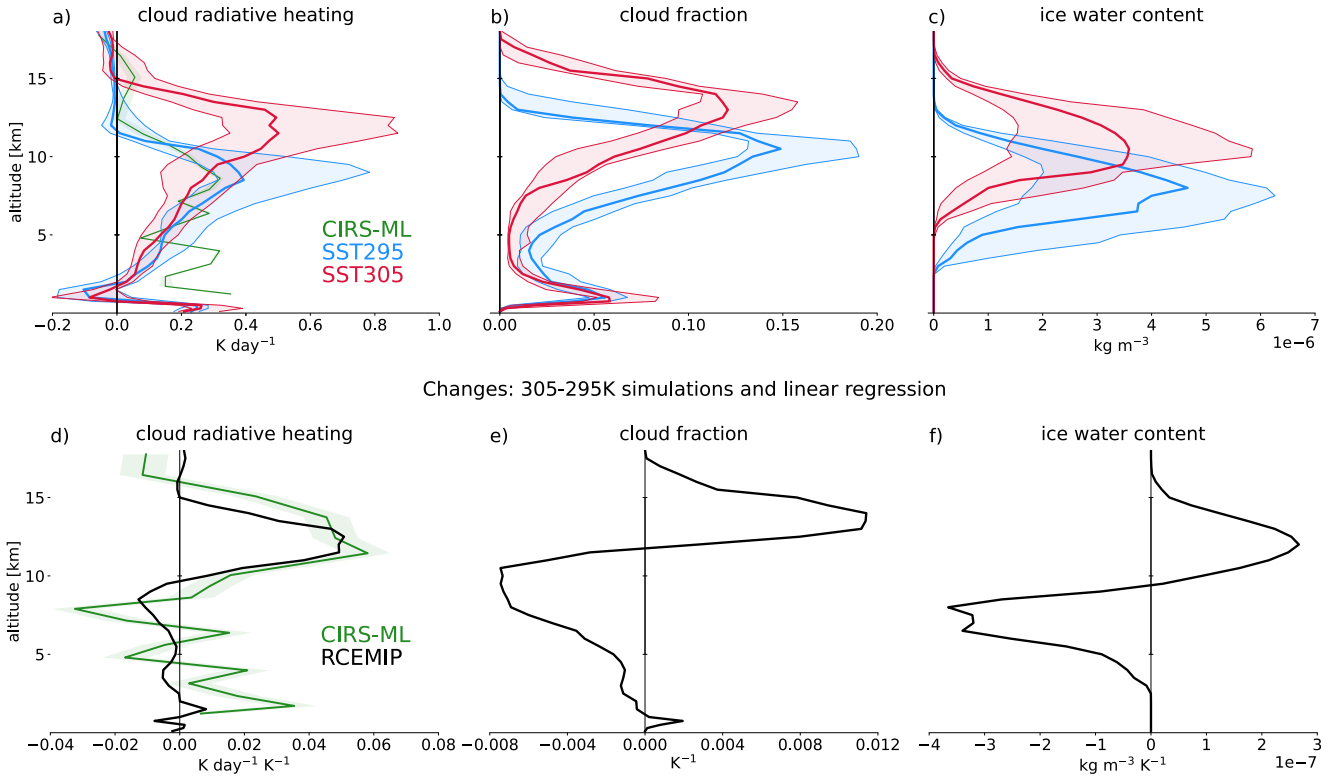

Figure 4. Median values (solid lines) and the interquartile range of RCEMIP model ensembles (shading) are shown for cloud radiative heating (a), cloud fraction (b), and IWC (c) in simulations with SSTs of 295 and 305 K. The green line in (a) shows the multiannual mean cloud radiative heating from CIRS-ML satellite retrievals; its maximum interannual range is represented by green shading (d)–(f) Illustrate changes between the median 305 and 295 K profiles for RCEMIP models (in black). In (d), the green line is the linear regression of CIRS-ML cloud radiative heating on tropical SST, with green shading for ±1 standard error.

3.4. Prediction of CRH Changes in RCEMIP

We now demonstrate that our prediction also works for a large ensemble of RCE model simulations from the RCEMIP project (Wing et al., 2018). Radiative (CRH), macrophysical (cloud fraction), and microphysical (IWC) properties clearly show high-cloud-related peaks that shift upward as the surface warms from 295 to 305 K (Figure 4). Similarly to SAM simulations, the model median CRH increases for a warmer atmosphere and surface, despite a decrease in cloud fraction and IWC (Figures 4a–4c and S4a–S4c in Supporting Information S1). Anomaly plots in temperature coordinates in Figures S4d–S4f in Supporting Information S1 highlight the changes between the colder and warmer simulations, with cloud fraction and IWC decreasing slightly while exhibiting nearly symmetrical altitude shifts (Figures 4d–4f). In contrast, the CRH increases in magnitude in the free troposphere and particularly near the peak high cloud fraction (Figure 4d and Figure S4d in Supporting Information S1).

We now apply the physical CRH prediction method developed based on the SAM model simulations to the RCEMIP data set, taking the 295 K simulations as the reference climate. Figure 5a supports our prediction for most RCEMIP cloud-resolving models (CRM), despite the large spread in simulated CRH profiles (Figure 4a). The isothermal vertical shift assumption alone explains on average 60% of the change in the CRH profiles between the 295 and 305 K simulations (brown bars in Figure S5 in Supporting Information S1; see Text S4 in Supporting Information S1 for details on calculations). The density adjustment increases the fraction of explained change by 10% (green bars in Figure S5 in Supporting Information S1), reducing the root mean square error of the prediction from 0.26 to 0.13 (Figure 5a). Peak CRH prediction is accurate within a 20% error for all but two analyzed CRMs, CM1 and NICAM (refer to Text S5 in Supporting Information S1 for explanation).

The interquartile range of the prediction error, averaged over all CRMs, is 0.1 K day^{-1} (Figure 5a). Model differences in the CRH change in response to surface warming are five times larger with 0.5 K day^{-1} (Figure 4a). Therefore, accurate prediction of CRH in a warmer climate requires a thorough understanding of its current state.

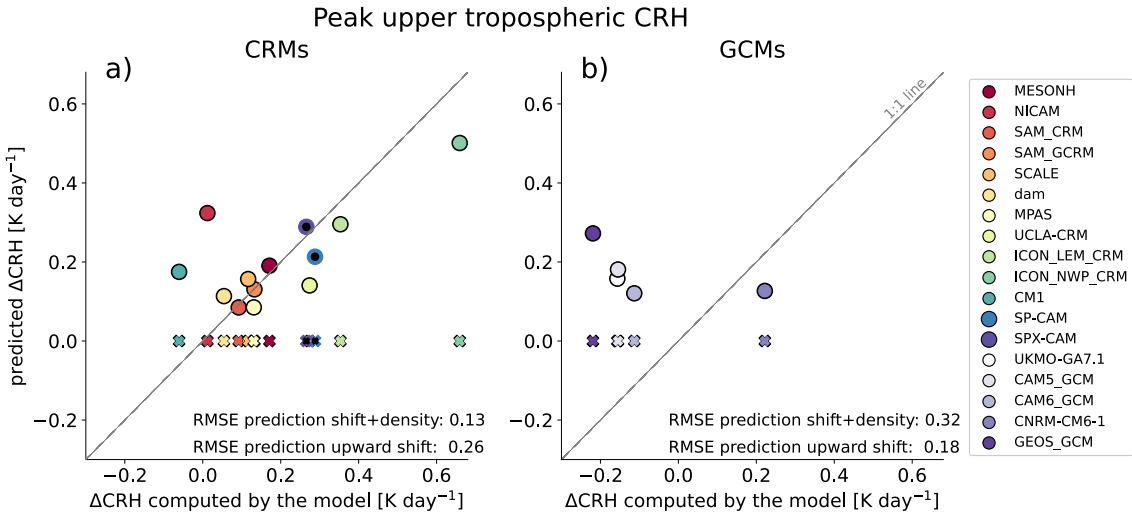

Figure 5. Predicted change in peak CRH (CRH_{305K}-CRH_{295K}) and its comparison with RCEMIP model-simulated values for (a) cloud-resolving models and (b) GCMs. Circles represent the full prediction, crosses the vertical shift of CRH with no change in magnitude. Symbols with black core highlight superparameterized models.

Our findings demonstrate that the prediction based on known physics is very powerful and explains 70% of the variation in CRH profiles for models with resolved deep convection (Figure 5 and Figure S5 in Supporting Information S1).

3.5. Density-Driven CRH Intensification in Satellite Estimates of CRH

We now show that our model results are comparable with CRH changes derived from satellite observations between 2004 and 2018. The upper tropospheric peak in CRH is located between 7 and 10 km, driven mainly by its LW component (green line in Figure 4a, Figures S6a–S6c in Supporting Information S1). The net CRH value at the cloud top is close to zero due to a cancellation between the LW cloud top emission and SW absorption (Figure 4a). The vertical profile of the observed CRH is more complex compared to the RCE simulations, with a larger contribution from mid- and low-level clouds. Moreover, cloud fraction and opacity are influenced by variations in SST (Figures S8, S9; Text S6 in Supporting Information S1). Most notably, the models simulate a warmer upper troposphere compared to observations. The RCEMIP output and the observations are therefore inconsistent in many climate properties, as described in Text S7 in Supporting Information S1. Nevertheless, the upper tropospheric CRH matches well between the satellite data set and the RCE simulations. This shows that RCE helps understand upper-tropospheric CRH in the tropics.

To study the response of CRH to increases in surface temperature, we use the annual tropical average SST and CRH anomalies relative to their time mean. The linear regression of the observation-based CRH profile with SST anomalies confirms the RCE results and our prediction that a warmer climate will lead to an asymmetric vertical shift of CRH, with stronger anomalous heating in the upper troposphere and weaker anomalous cooling in the middle troposphere (Figure 4d, green line).

Given the similarity between the observations and RCE simulations, the satellite observations provide a fourth line of evidence for the strengthening of upper tropospheric CRH in warmer climate conditions.

4. Implications for Climate Modeling

Our analysis so far has used only models with kilometer-scale grid spacing and an explicit treatment of deep convection. However, general circulation models (GCMs) are critical for climate projections, despite their limited ability to capture subgrid-scale processes like deep convection. Therefore, we present a separate analysis of changes in simulated CRH from GCMs in the RCE data set. In contrast to CRMs, our prediction of changes in CRH with warming cannot capture the GCM responses in a satisfactory way (Figure 5b).

We reveal substantial discrepancies between their responses to warming and the predictions based on fundamental atmospheric thermodynamics and CRM simulations. For example, analyzed GCMs often produce large

changes in IWC in warmer climates (Figure S7 in Supporting Information S1), for which there is no physical justification based on atmospheric thermodynamics (Sokol & Hartmann, 2022). These changes in IWC dominate the change in upper tropospheric CRH, raising questions about the reliability of models with parameterized deep convection for accurate climate predictions.

Our analysis also highlights the potential of models with embedded CRMs, such as the SP-CAM and SPX-CAM versions of the CAM model, to improve the accuracy of simulating clouds and their CRH. By bypassing the need for convective parameterization, these models produce results that align with the physical understanding of the tropical atmosphere and our predicted response to warming despite having similarly coarse vertical grid spacing as GCM versions of the CAM model (Figures S5 and S7 in Supporting Information S1). While the discrepancies between GCMs and basic physical understanding are concerning, the emergence of global CRMs presents an exciting opportunity to advance our understanding of the climate system and improve the accuracy of climate projections (Hohenegger et al., 2023; Satoh et al., 2014).

5. Summary and Implications

We show that the strength of cloud-radiative interactions in high clouds changes primarily as a function of air density. The decrease in air density causes an increase in the magnitude of CRH, which we find to operate in radiative transfer calculations of an idealized high cloud, simulations with SAM over a broad range of SSTs, a multimodel simulation data set of RCE, and a 15-year satellite-derived data set. In the RCE simulations, this density-driven CRH increase, on average, overcompensates for the effect of a decreasing high cloud fraction (Bony et al., 2016).

Using a theory of dilute moist adiabatic ascent and fixed high cloud temperature, we can predict simulated CRH responses to warming with good accuracy. Remarkably, the prediction is skillful for most CRMs despite the large spread of model-simulated CRH profiles under present-day-like conditions (Figures 4a and 5a). Knowledge of changes in upper tropospheric cloud fraction and/or condensate could further improve the prediction. A predictive cloud fraction equation may be derived by building upon the work by Jeevanjee (2022) and Beydoun et al. (2021).

Recent work using GCMs in a realistic setup showed that CRH response to a 4K warmer SST can be largely explained by an upward shift only (Voigt et al., 2024). This is not the case in the RCEMIP GCM simulations. In contrast, GCMs simulate large changes in cloud properties, particularly IWC, in response to warming. These changes drive most of the response in upper tropospheric CRH, violating the simple physics on which our CRH prediction method is based. Such changes in cloud properties are likely related to uncertain deep convective parameterizations and should be approached with caution.

Observational studies have shown altitude shifts of clouds in response to warmer temperatures based on inter-annual climate variability (e.g., Zelinka & Hartmann, 2011) and observed global mean warming (Norris et al., 2016). These findings suggest that the altitude-driven CRH change may already influence the role of high clouds in the climate system. In particular, these changes are likely affecting the planetary-scale circulation of the atmosphere, the location of strong precipitation as well as the life cycle of upper tropospheric clouds.

Our study demonstrates that by using well-established principles of atmospheric physics, convection, and clouds, it is possible to reliably predict the response of CRH to surface warming for a wide range of climates. Our findings suggest that more effort should be devoted to calibrating models using satellite-derived CRH. Indeed, our results indicate that the uncertainty in model-predicted changes in atmospheric circulations and hence regional climate could be significantly reduced by narrowing the spread in model-simulated CRH in the present-day climate. This is an avenue for progress that climate modeling has largely overlooked so far.

Data Availability Statement

RCEMIP output is hosted by the German Climate Computing Center (DKRZ), available at Wing, Stauffer, Becker, Reed, Ahn, Arnold, and Zhao (2020). NOAA OI SST data set is available at https://psl.noaa.gov/data/gridded/data.noaa.oisst.v2.highres.html. CIRS data set is available at https://gewex-utcc-proes.aeris-data.fr/data/ (last access: 22 August 2024). The data, analysis, and plotting scripts are found in Gasparini et al. (2024).

Acknowledgments
Thanks to Dennis Hartmann for the SPM code, Adam Sokol for the SAM modifications needed to replicate the RCEMIP setup, Jiawei Bao, Brett McKim, Lukas Brunner, Vanessa Rieger for discussions/comments. BG and AV acknowledge funding from the European Union's Horizon 2020 research and innovation programme under the Marie Skłodowska-Curie grant agreement No 101025473. CS and GM acknowledge CNES and CNRS for funding. Computational results were achieved in part using the Vienna Scientific Cluster (VSC).

References

Ackerman, T. P., Liou, K.-N., Valero, P. J. F., & Pfister, L. (1988). Heating rates in tropical anvils. *Journal of the Atmospheric Sciences*, *45*(10), 1606–1623. https://doi.org/10.1175/1520-0469(1988)045⟨1606:HRITA⟩2.0.CO;2

Albern, N., Voigt, A., Buehler, S. A., & Grützun, V. (2018). Robust and non-robust impacts of atmospheric cloud-radiative interactions on the tropical circulation and its response to surface warming. *Geophysical Research Letters*, *45*(16), 8577–8585. https://doi.org/10.1029/2018GL079599

Beydoun, H., Caldwell, P. M., Hannah, W. M., & Donahue, A. S. (2021). Dissecting anvil cloud response to Sea Surface warming. *Geophysical Research Letters*, *48*(15), e2021GL094049. https://doi.org/10.1029/2021GL094049

Bony, S., Stevens, B., Coppin, D., Becker, T., Reed, K. A., Voigt, A., & Medeiros, B. (2016). Thermodynamic control of anvil cloud amount. *Proceedings of the National Academy of Sciences*, *113*(32), 8927–8932. https://doi.org/10.1073/pnas.1601472113

Byrne, M. P., & Zanna, L. (2020). Radiative effects of clouds and water Vapor on an axisymmetric monsoon. *Journal of Climate*, *33*(20), 8789–8811. https://doi.org/10.1175/JCLI-D-19-0974.1

Ceppi, P., & Hartmann, D. L. (2016). Clouds and the atmospheric circulation response to warming. *Journal of Climate*, *29*(2), 783–799. https://doi.org/10.1175/JCLI-D-15-0394.1

Ceppi, P., & Shepherd, T. G. (2017). Contributions of climate feedbacks to changes in atmospheric circulation. *Journal of Climate*, *30*(22), 9097–9118. https://doi.org/10.1175/JCLI-D-17-0189.1

Dee, D. P., Uppala, S. M., Simmons, A. J., Berrisford, P., Poli, P., Kobayashi, S., et al. (2011). The ERA-Interim reanalysis: Configuration and performance of the data assimilation system. *Quarterly Journal of the Royal Meteorological Society*, *137*(656), 553–597. https://doi.org/10.1002/qj.828

Dinh, T., Gasparini, B., & Bellon, G. (2023). Clouds and radiatively induced circulations. In S. C. Sullivan & C. Hoose (Eds.), *Cloud physics and dynamics: Showers and shade from earth's atmosphere* (pp. 239–253). American Geophysical Union Monograph Series.

Gasparini, B., Blossey, P. N., Hartmann, D. L., Lin, G., & Fan, J. (2019). What drives the life cycle of tropical anvil clouds? *Journal of Advances in Modeling Earth Systems*, *11*(9), 2586–2605. https://doi.org/10.1029/2019MS001736

Gasparini, B., Mandorli, G., Stubenrauch, C., & Voigt, A. (2024). Data and Scripts for "Basic physics predicts stronger high cloud radiative heating with warming"[Collection]. *Zenodo*. https://doi.org/10.5281/zenodo.13951361

Gasparini, B., Sokol, A. B., Wall, C. J., Hartmann, D. L., & Blossey, P. N. (2022). Diurnal differences in tropical maritime anvil cloud evolution. *Journal of Climate*, *35*(5), 1655–1677. https://doi.org/10.1175/jcli-d-21-0211.1

Harrop, B. E., & Hartmann, D. L. (2016a). The role of cloud radiative heating in determining the location of the ITCZ in aquaplanet simulations. *Journal of Climate*, *29*(8), 2741–2763. https://doi.org/10.1175/JCLI-D-15-0521.1

Harrop, B. E., & Hartmann, D. L. (2016b). The role of cloud radiative heating within the atmosphere on the high cloud amount and top-of-atmosphere cloud radiative effect. *Journal of Advances in Modeling Earth Systems*, *8*(3), 1391–1410. https://doi.org/10.1002/2016MS000670

Hartmann, D. L., Dygert, B. D., Blossey, P. N., Fu, Q., & Sokol, A. B. (2022). The vertical profile of radiative cooling and lapse rate in a warming climate. *Journal of Climate*, *35*(19), 2653–2665. https://doi.org/10.1175/JCLI-D-21-0861.1

Hartmann, D. L., Gasparini, B., Berry, S. E., & Blossey, P. N. (2018). The life cycle and net radiative effect of tropical anvil clouds. *Journal of Advances in Modeling Earth Systems*, *10*(12), 3012–3029. https://doi.org/10.1029/2018MS001484

Hartmann, D. L., & Larson, K. (2002). An important constraint on tropical cloud - Climate feedback. *Geophysical Research Letters*, *29*(20), 1951. https://doi.org/10.1029/2002GL015835

Haslehner, K., Gasparini, B., & Voigt, A. (2024). Radiative heating of high-level clouds and its impacts on climate. *Journal of Geophysical Research: Atmospheres*, *129*(12), e2024JD040850. https://doi.org/10.1029/2024JD040850

Henderson, D. S., L'Ecuyer, T., Stephens, G., Partain, P., & Sekiguchi, M. (2013). A multisensor perspective on the radiative impacts of clouds and aerosols. *Journal of Applied Meteorology and Climatology*, *52*(4), 853–871. https://doi.org/10.1175/JAMC-D-12-025.1

Hohenegger, C., Korn, P., Linardakis, L., Redler, R., Schnur, R., Adamidis, P., et al. (2023). ICON-Sapphire: Simulating the components of the Earth system and their interactions at kilometer and subkilometer scales. *Geoscientific Model Development*, *16*(2), 779–811. https://doi.org/10.5194/gmd-16-779-2023

Höjgård-Olsen, E., Chepfer, H., & Brogniez, H. (2022). Satellite observed sensitivity of tropical clouds and moisture to Sea Surface temperature on various time and space scales: 1. Focus on high level cloud situations over ocean. *Journal of Geophysical Research: Atmospheres*, *127*(6), e2021JD035438. https://doi.org/10.1029/2021JD035438

Huang, B., Liu, C., Banzon, V., Freeman, E., Graham, G., Hankins, B., et al. (2021). Improvements of the daily Optimum Interpolation Sea Surface temperature (DOISST) version 2.1. *Journal of Climate*, *34*(8), 2923–2939. https://doi.org/10.1175/JCLI-D-20-0166.1

Iacono, M. J., Delamere, J. S., Mlawer, E. J., Shephard, M. W., Clough, S. A., & Collins, W. D. (2008). Radiative forcing by long-lived greenhouse gases: Calculations with the AER radiative transfer models. *Journal of Geophysical Research*, *113*(13), 2–9. https://doi.org/10.1029/2008JD009944

Jeevanjee, N. (2022). Three rules for the decrease of tropical convection with global warming. *Journal of Advances in Modeling Earth Systems*, *14*(11), e2022MS003285. https://doi.org/10.1029/2022MS003285

Jeevanjee, N., & Fueglistaler, S. (2020). Simple spectral models for atmospheric radiative cooling. *Journal of the Atmospheric Sciences*, *77*(2), 479–497. https://doi.org/10.1175/JAS-D-18-0347.1

Khairoutdinov, M. F., & Randall, D. A. (2003). Cloud resolving modeling of the ARM summer 1997 IOP: Model formulation, results, uncertainties, and sensitivities. *Journal of the Atmospheric Sciences*, *60*(4), 607–625. https://doi.org/10.1175/1520-0469(2003)060⟨0607:CRMOTA⟩2.0.CO;2

Knutson, T. R., & Manabe, S. (1995). Time-mean response over the tropical Pacific to increased C02 in a coupled ocean-atmosphere model. *Journal of Climate*, *8*(9), 2181–2199. https://doi.org/10.1175/1520-0442(1995)008⟨2181:TMROTT⟩2.0.CO;2

Li, Y., Thompson, D. W. J., & Bony, S. (2015). The influence of atmospheric cloud radiative effects on the large-scale atmospheric circulation. *Journal of Climate*, *28*(18), 7263–7278. https://doi.org/10.1175/JCLI-D-14-00825.1

Li, Y., Thompson, D. W. J., Bony, S., & Merlis, T. M. (2019). Thermodynamic control on the poleward shift of the extratropical jet in climate change simulations: The role of rising high clouds and their radiative effects. *Journal of Climate*, *32*(3), 917–934. https://doi.org/10.1175/JCLI-D-18-0417.1

Li, Y., Yang, P., North, G. R., & Dessler, A. (2012). Test of the fixed anvil temperature hypothesis. *Journal of the Atmospheric Sciences*, *69*(7), 2317–2328. https://doi.org/10.1175/JAS-D-11-0158.1

Lohmann, U., & Roeckner, E. (1995). Influence of cirrus cloud radiative forcing on climate and climate sensitivity in a general circulation model. *Journal of Geophysical Research*, *100*(D8), 16305–16323. https://doi.org/10.1029/95JD01383

Medeiros, B., Clement, A. C., Benedict, J. J., & Zhang, B. (2021). Investigating the impact of cloud-radiative feedbacks on tropical precipitation extremes. *npj Climate and Atmospheric Science*, *4*(1), 1–10. https://doi.org/10.1038/s41612-021-00174-x

Mitchell, J. F. B., & Ingram, W. J. (1992). Carbon dioxide and climate: Mechanisms of changes in cloud. *Journal of Climate*, *5*(1), 5–21. https://doi.org/10.1175/1520-0442(1992)005⟨0005:CDACMO⟩2.0.CO;2

Mlawer, E. J., Taubman, J., Brown, P. D., Iacono, M. J., & Clough, S. A. (1997). Radiative transfer for inhomogeneous atmospheres: RRTM, a validated correlated-k model for the longwave. *Journal of Geophysical Research*, *102*(D14), 16663–16682. https://doi.org/10.1029/97JD00237

Muller, C., Yang, D., Craig, G., Cronin, T., Fildier, B., Haerter, J. O., et al. (2022). Spontaneous aggregation of convective storms. *Annual Review of Fluid Mechanics*, *54*(1), 133–157. https://doi.org/10.1146/annurev-fluid-022421-011319

Norris, J. R., Allen, R. J., Evan, A. T., Zelinka, M. D., O'Dell, C. W., & Klein, S. A. (2016). Evidence for climate change in the satellite cloud record. *Nature*, *536*(7614), 72–75. https://doi.org/10.1038/NATURE18273

Po-Chedley, S., Zelinka, M. D., Jeevanjee, N., Thorsen, T. J., & Santer, B. D. (2019). Climatology explains intermodel spread in tropical upper tropospheric cloud and relative humidity response to greenhouse warming. *Geophysical Research Letters*, *46*(22), 13399–13409. https://doi.org/10.1029/2019GL084786

Pope, K. N., Holloway, C. E., Jones, T. R., & Stein, T. H. M. (2021). Cloud-radiation interactions and their contributions to convective self-aggregation. *Journal of Advances in Modeling Earth Systems*, *13*(9), e2021MS002535. https://doi.org/10.1029/2021MS002535

Rädel, G., Mauritsen, T., Stevens, B., Dommenget, D., Matei, D., Bellomo, K., & Clement, A. (2016). Amplification of El Niño by cloud longwave coupling to atmospheric circulation. *Nature Geoscience*, *9*(2), 106–110. https://doi.org/10.1038/ngeo2630

Ramanathan, V., Pitcher, E. J., Malone, R. C., & Blackmon, M. L. (1983). The response of a spectral general circulation model to refinements in radiative processes. *Journal of the Atmospheric Sciences*, *40*(3), 605–630. https://doi.org/10.1175/1520-0469(1983)040⟨0605:TROASG⟩2.0.CO;2

Ruppert, J. H., Wing, A. A., Tang, X., & Duran, E. L. (2020). The critical role of cloud–infrared radiation feedback in tropical cyclone development. *Proceedings of the National Academy of Sciences of the United States of America*, *117*(45), 27884–27892. https://doi.org/10.1073/pnas.2013584117

Satoh, M., Tomita, H., Yashiro, H., Miura, H., Kodama, C., Seiki, T., et al. (2014). The non-hydrostatic icosahedral atmospheric model: Description and development. *Progress in Earth and Planetary Science*, *1*(1), 18. https://doi.org/10.1186/s40645-014-0018-1

Seeley, J. T., Jeevanjee, N., Langhans, W., & Romps, D. M. (2019). Formation of tropical anvil clouds by slow evaporation. *Geophysical Research Letters*, *46*(1), 492–501. https://doi.org/10.1029/2018GL080747

Sherwood, S. C., Webb, M. J., Annan, J. D., Armour, K. C., Forster, P. M., Hargreaves, J. C., et al. (2020). An assessment of Earth's climate sensitivity using multiple lines of evidence. *Reviews of Geophysics*, *58*(4), 1–92. https://doi.org/10.1029/2019rg000678

Singh, M. S., & O'Gorman, P. A. (2015). Increases in moist-convective updraught velocities with warming in radiative-convective equilibrium. *Quarterly Journal of the Royal Meteorological Society*, *141*(692), 2828–2838. https://doi.org/10.1002/qj.2567

Sokol, A. B., & Hartmann, D. L. (2020). Tropical anvil clouds: Radiative driving toward a preferred state. *Journal of Geophysical Research: Atmospheres*, *125*(21), e2020JD033107. https://doi.org/10.1029/2020JD033107

Sokol, A. B., & Hartmann, D. L. (2022). Congestus mode invigoration by convective aggregation in simulations of radiative-convective equilibrium. *Journal of Advances in Modeling Earth Systems*, *14*(7), e2022MS003045. https://doi.org/10.1029/2022MS003045

Stubenrauch, C. J., Caria, G., Protopapadaki, S. E., & Hemmer, F. (2021). 3D radiative heating of tropical upper tropospheric cloud systems derived from synergistic A-Train observations and machine learning. *Atmospheric Chemistry and Physics*, *21*(2), 1015–1034. https://doi.org/10.5194/acp-21-1015-2021

Stubenrauch, C. J., Feofilov, A. G., Protopapadaki, S. E., & Armante, R. (2017). Cloud climatologies from the infrared sounders AIRS and IASI: Strengths and applications. *Atmospheric Chemistry and Physics*, *17*(22), 13625–13644. https://doi.org/10.5194/acp-17-13625-2017

Stubenrauch, C. J., Mandorli, G., & Lemaitre, E. (2023). Convective organization and 3D structure of tropical cloud systems deduced from synergistic A-Train observations and machine learning. *Atmospheric Chemistry and Physics*, *23*(10), 5867–5884. https://doi.org/10.5194/acp-23-5867-2023

Takahashi, H., Luo, Z. J., Masunaga, H., Storer, R., & Noda, A. T. (2024). Investigating convective processes underlying ENSO: New insights into the fixed anvil temperature hypothesis. *Geophysical Research Letters*, *51*(6), e2023GL107113. https://doi.org/10.1029/2023GL107113

Thompson, D. W., Bony, S., & Li, Y. (2017). Thermodynamic constraint on the depth of the global tropospheric circulation. *Proceedings of the National Academy of Sciences of the United States of America*, *114*(31), 8181–8186. https://doi.org/10.1073/pnas.1620493114

Voigt, A., & Albern, N. (2019). No cookie for climate change. *Geophysical Research Letters*, *46*(24), 14751–14761. https://doi.org/10.1029/2019GL084987

Voigt, A., Albern, N., Ceppi, P., Grise, K., Li, Y., & Medeiros, B. (2021). Clouds, radiation, and atmospheric circulation in the present-day climate and under climate change. *Wiley Interdisciplinary Reviews: Climate Change*, *12*(2), 1–22. https://doi.org/10.1002/wcc.694

Voigt, A., North, S., Gasparini, B., & Ham, S.-H. (2024). Atmospheric cloud-radiative heating in CMIP6 and observations and its response to surface warming. *Atmospheric Chemistry and Physics*, *24*(17), 9749–9775. https://doi.org/10.5194/acp-24-9749-2024

Voigt, A., & Shaw, T. A. (2015). Circulation response to warming shaped by radiative changes of clouds and water vapour. *Nature Geoscience*, *8*(2), 102–106. https://doi.org/10.1038/ngeo2345

Voigt, A., & Shaw, T. A. (2016). Impact of regional atmospheric cloud radiative changes on shifts of the extratropical jet stream in response to global warming. *Journal of Climate*, *29*(23), 8399–8421. https://doi.org/10.1175/JCLI-D-16-0140.1

Wall, C. J., Norris, J. R., Gasparini, B., Smith, W. L., Thieman, M. M., & Sourdeval, O. (2020). Observational evidence that radiative heating modifies the life cycle of tropical anvil clouds. *Journal of Climate*, *33*(20), 8621–8640. https://doi.org/10.1175/JCLI-D-20-0204.1

Wing, A. A., Reed, K. A., Satoh, M., Stevens, B., Ohno, T., & Bony, S. (2018). Radiative–convective equilibrium model intercomparison project. *Geoscientific Model Development*, *11*(2), 793–813. https://doi.org/10.5194/gmd-11-793-2018

Wing, A. A., Stauffer, C. L., Becker, T., Reed, K. A., Ahn, M. S., Arnold, N. P., et al. (2020). Clouds and convective self-aggregation in a multimodel ensemble of radiative-convective equilibrium simulations. *Journal of Advances in Modeling Earth Systems*, *12*(9), 1–38. https://doi.org/10.1029/2020MS002138

Wing, A. A., Stauffer, C. L., Becker, T., Reed, K. A., Ahn, M.-S., Arnold, N. P., et al. (2020b). RCEMIP data [Dataset]. http://hdl.handle.net/21.14101/d4beee8e-6996-453e-bbd1-ff53b6874c0e

Zelinka, M. D., & Hartmann, D. L. (2011). The observed sensitivity of high clouds to mean surface temperature anomalies in the tropics. *Journal of Geophysical Research*, *116*(23), 1–16. https://doi.org/10.1029/2011JD016459

Zhou, C., Dessler, A., Zelinka, M., Yang, P., & Wang, T. (2014). Cirrus feedback on interannual climate fluctuations. *Geophysical Research Letters*, *41*(24), 9166–9173. https://doi.org/10.1002/2014GL062095

Zhou, W., & Xie, S.-P. (2019). A conceptual spectral plume model for understanding tropical temperature profile and convective updraft velocities. *Journal of the Atmospheric Sciences*, *76*(9), 2801–2814. https://doi.org/10.1175/JAS-D-18-0330.1